Tiago Rodrigues, J. G. Pinto, Vítor Monteiro, Delfim Pedrosa, João L. Afonso,

“Renewable Energy System for an Isolated Micro Grid”

IEEE IECON Industrial Electronics Conference, pp.1636-1642, Dallas Texas USA, Oct. 2014.

http://ieeexplore.ieee.org/stamp/stamp.jsp?tp=&arnumber=7048811&tag=1

ISBN: 978-1-4799-4033-2

ISSN: 1553-572X

DOI 10.1109/IECON.2014.7048811

Tiago Rodrigues, J. G. Pinto, Vítor Monteiro, Delfim Pedrosa, João L. Afonso, "Renewable Energy System for an Isolated Micro Grid", IEEE IECON Industrial Electronics Conference, pp. 2226-2232, Dallas Texas USA, Oct. 2014, ISBN: 978-1-4799-4033-2, ISSN: 1553-572X, DOI:10.1109/IECON.2014.7048811

Renewable Energy System for an Isolated Micro Grid

Tiago Rodrigues, J. G. Pinto, Vitor Monteiro, João L. Afonso
ALGORITMI Research Centre – University of Minho – Guimarães, Portugal
{tiago.rodrigues | gabriel.pinto | vitor.monteiro | joao.l.afonso}@algoritmi.uminho.pt

***Abstract*—This paper presents the development of the power electronics needed for the interaction between the electrical generator of a wind turbine and an isolated ac micro grid. In this system there are basically two types of receptors for the energy produced by the wind turbine, which are the loads connected to the isolated micro grid and the batteries used to store energy. There are basically two states in which the system will work. One of the states is when there is enough wind power to supply the loads and the extra energy is used to charge the batteries. The other state is when there is low wind power and the batteries have to compensate the lack of power, so that the isolated micro grid has enough power to supply at least the priority loads. In this paper are presented the hardware and the control algorithm for the developed system. The topology was previously tested in computer simulations, using the software PSIM 9.0, and then validated with the implementation of a laboratory prototype.**

Keywords—Renewable Energy System, Isolated Micro Grid, Power Electronics, Wind Power

I. INTRODUCTION

In order to reduce fossil fuels dependency in the production of electrical energy, there has been an increase in the installation of renewable energies [1]. Since 2000, wind, photovoltaic solar and gas installed power has increased 115.4 GW, 80 GW and 131.7 GW, respectively. On the other hand, fuel oil, coal and nuclear installed power sources have decreased 28.7 GW, 19 GW and 8.5 GW, respectively [2]. The main reason for these changes is the fact that the renewable energies have a clean production and so, there is no production of residual products that fossil energy sources produce [3]. Also, renewable energies are an unlimited source of energy, contrasting with fossil fuels, which, for example, oil, is starting to grow scarce.

The wind power is a source of energy that has been increasing in its installed power around the world [4]. It is mainly used in grid tied applications, where the energy extracted from the wind is injected in the power grid [5][6]. There is another kind of application to this type of energy source, which is an off-grid system, also known as isolated system. In this system, the energy provided by the wind system must satisfy the needs of the loads connected to a micro grid. However, since this system is dependent on one source of energy that is not constant, batteries are used to smooth the intermittent energy produced by the wind turbine, therefore making possible to power the micro grid even when there is no wind. Additionally, this system can be complemented with another type of energy source, for example, photovoltaic solar energy or a diesel engine-generator system [7]. This makes the system more stable since it has another reliable energy source to compensate the lack of wind, turning the system into a hybrid one [8]. Since the micro grid is reliant on the energy generated by the sources connected to it and the batteries that are used to store the extra produced energy, there can be moments in which the available energy will be lower than required, leading to a need to disable some lower priority loads to save energy [9]. All of these factors need to be taken in account when designing the system. These off-grid systems are normally used when extending the main grid to the desired location is more expensive compared to creating a micro grid to satisfy those needs [10]. The existing micro grids are normally composed by a diesel engine-generator source, however as most of these zones are of difficult access, the transportation of the required fuel can pose a problem. In addition, the noise caused can also become a disturbance. The problem is reduced by the introduction of renewable energies [11]. Comparing the quality of the energy produced by these two sources, as the renewable energies use controlled power electronics inverters they are less affected by the variation of loads, producing a voltage with better quality compared to the diesel engine-generator systems [12].

In terms of power electronics converters for micro-wind turbines several topologies have been proposed. In [13], it is presented a single-phase topology for energy extraction from wind turbines. However, this type of topology is not suitable to work in isolated mode, since there is no device that can store energy, making the system unreliable. In [14], it is proposed another topology, this one though, works in isolated systems, but is not ideal when generators with high voltage output and low voltage batteries are used, since the dc-dc buck-boost converter is not suitable to reduce the voltage from high levels to low levels. Fig. 1 shows a block diagram of the proposed micro-wind system. The ac voltage produced by the electrical generator is converted to dc by a rectifier. The full-bridge

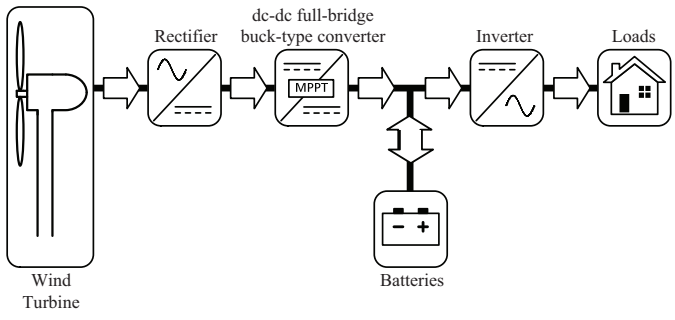

Fig. 1. Micro-wind isolated system block diagram.

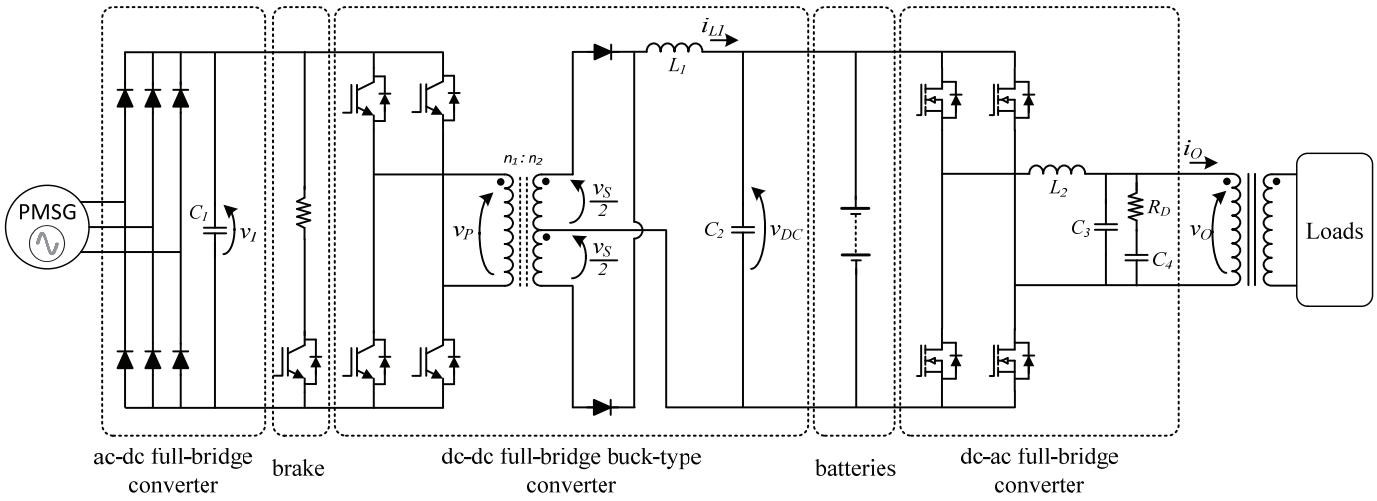

Fig. 2. Electrical diagram of the proposed micro-wind isolated system.

buck-type dc-dc converter optimizes the energy extraction and manages the batteries charging. This type of converter is normally used in high power systems, allowing a better control over the level of the voltage in the output [15]. The inverter is used to produce a sinusoidal voltage with the desired frequency and amplitude to supply the loads.

II. System Architecture

In this item, it is presented the system architecture used in the current application. As shown in Fig. 2 this system is composed by three power converters: an ac-dc bridge rectifier; a dc-dc full-bridge buck-type; and a dc-ac full-bridge. The ac-dc bridge rectifier is only used to convert the ac voltage from the generator to a dc voltage. Furthermore, the dc-dc full-bridge buck-type converter is used to convert the voltage from the output of the ac-dc converter to the desired level, which will be applied to charge the batteries. Finally, the dc-ac full-bridge converter is used to convert the dc link voltage to a low distortion sinusoidal voltage with the desired amplitude and frequency. A more detailed analysis of these converters is further presented.

Besides the three converters, the system is also composed by a permanent magnet synchronous generator (PMSG), which the output voltage and maximum power is a function of the wind velocity. To prevent that the generator reaches rotational velocities greater than the nominal it is used an electrical brake system. This system is activated when the wind turbine velocity reaches a certain value in which it can damage the generator or other mechanical components. Also, when the batteries are fully charged and the energy produced by the generator is superior to what is needed by the loads, the brake will also serve as a mean to dissipate the incoming energy. It is also used an output transformer to adapt the voltage that is applied to the loads, which is necessary due to the batteries low voltage.

A. Dc-dc Full-Bridge Buck-Type Converter

This section presents the description of the dc-dc full-bridge buck-type converter. The objective of this converter is the regulation of the dc link voltage (v_{DC}), which at the same time allows the implementation of the maximum power point tracker (MPPT) control algorithm. This converter is controlled by applying PWM signals to the IGBTs in order to produce a square output voltage with variable duty-cycle in the full-bridge output. These PWM signals are created by comparing the voltage reference with a high frequency triangular carrier waveform. The output voltage amplitude of this converter will be reduced by the high-frequency transformer with center-tapped secondary winding. The transformer secondary winding is connected to a two diode full-wave voltage rectifier to obtain a positive voltage. The output voltage can be calculated with (1).

$$v_{DC} = \frac{v_I \, \delta}{2n}, \tag{1}$$

in which v_{DC} is the output voltage, v_I the input voltage, δ the duty-cycle of the output voltage of the high-frequency transformer and n the relation of turns of the transformer. Fig. 3 shows the simulation results of this converter. In Fig. 3 (a) it is shown the voltage (v_P) applied to the high-frequency transformer and its secondary output voltage (v_S), for an input voltage (v_I) of 90V and a duty-cycle (δ) of 50%. In Fig. 3 (b) it is shown the output voltage of the converter (v_{DC}) and the current in the inductor (i_{L1}) in continuous conduction mode. It is possible to observe that the current in the inductor varies in accordance with the voltage applied to it, never getting to zero. In this application it is important to have a transformer with low leakage inductance in order to avoid duty-cycle related problems of the voltage in the secondary of the transformer, which would lead to a voltage lower than expected in the output of the converter.

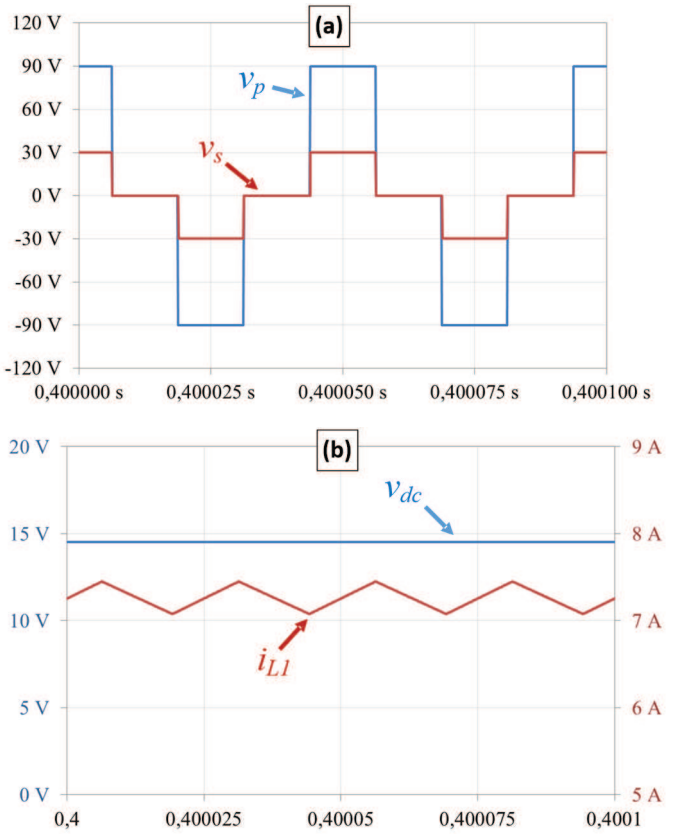

Fig. 3. Simulation results of the dc-dc full-bridge buck-type converter: (a) Primary voltage (v_p) and secondary voltage (v_s); (b) Dc link voltage (v_{DC}) and inductor current (i_{L1}).

As aforementioned, besides regulating the output voltage, this converter must also implement a MPPT control algorithm aiming to extract the maximum power that the generator can produce in function of the wind speed.

Two different types of MPPT were evaluated: power signal feedback; and perturbation and observation. The power signal feedback permits a better control over the current and also a better efficiency in the extraction of power. Nevertheless, this control needs the power curve of the generator, which can be considered a drawback. The perturbation and observation is a more basic control, which permits the extraction of the maximum power with acceptable efficiency. This control does not need any information about the generator and so permits an easier use. The results presented in this work are achieved with the perturbation observation algorithm. This control applies a step variation (perturbation) in the duty-cycle of the dc-dc converter and observes how the system reacts. The imposed perturbation on the duty-cycle can be positive or negative. If after a positive perturbation the extracted power increases, the next perturbation will be in the same way (incrementing again the duty-cycle). Else if the extracted power reduces, negative perturbations (reductions in the duty-cycle) will be applied while the extracted power increases. With this algorithm the extracted power follows the maximum available power. Fig. 4 shows the flowchart of the perturbation and observation MPPT

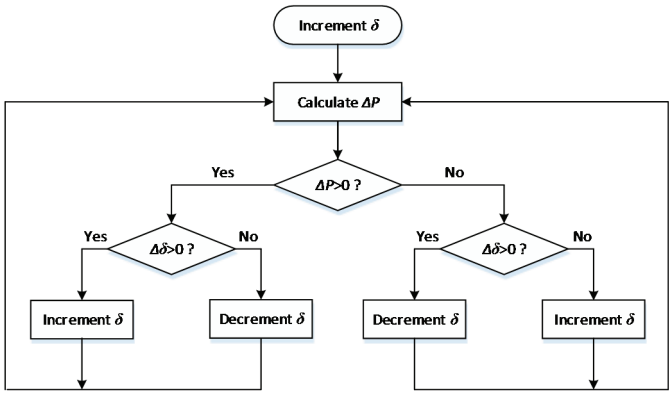

Fig. 4. Flowchart of the Perturbation and Observation MPPT control algorithm.

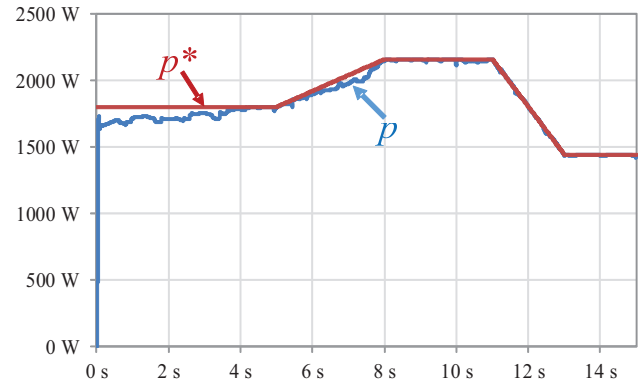

Fig. 5. Simulation results of the extracted power (p) and the maximum theoretical power of the generator (p^*) for different wind speeds.

algorithm. In Fig. 5 it is shown the obtained results using the aforementioned algorithm. It is possible to verify that the extracted power (p) follows the theoretical maximum power possible to extract from the generator (p^*) for different wind speeds.

B. Dc-ac Full-Bridge Converter

This section presents the description of the dc-ac full-bridge converter. This converter in addition with an output transformer allows the conversion of the voltage from the dc link to an ac voltage with 230 V RMS and 50 Hz of frequency that will be applied to the loads. The switching technique used in this converter to obtain the pulses pattern applied to the MOSFETs was the unipolar synchronized pulse-width modulation (SPWM). This technique consists in comparing a high frequency triangular carrier waveform with a sinusoidal waveform reference for one of the legs of the converter, and another sinusoidal reference lagged by 180º to the other leg. The result of each comparison is applied to the top MOSFET and the result negated is applied to the other MOSFET in the same leg. In theory, the reference will be a sinusoidal waveform and its frequency will be equal to the frequency desired to the output voltage. The amplitude of output voltage can be calculated by using (2).

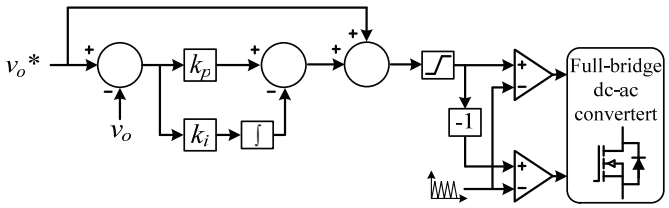

Fig. 6. Diagram of the dc-ac converter control.

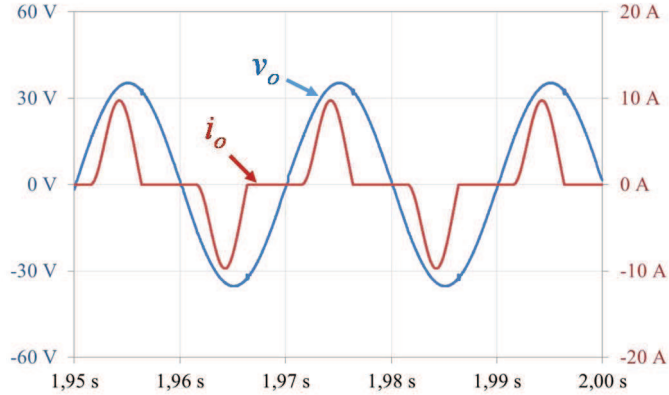

Fig. 7. Simulation results of the dc-ac converter: output voltage (v_o) and output current (i_o).

$$V_{OP} = m_a * v_{DC}\,, \tag{2}$$

where, V_{OP} is the amplitude of the output voltage, and m_a the modulation index, which is calculated by:

$$m_a = \frac{V_{RP}}{V_{TP}}, \tag{3}$$

in which, V_{TP} is the maximum amplitude of the triangular carrier waveform, and V_{RP} the maximum amplitude of the reference signal waveform. It is important refer that the V_{TP} must have the same amplitude of the dc-link voltage. In practice, it is needed a dead-time between the control signals of a given converter leg to avoid a short circuit during the switching of the MOSFETs. However, introducing this dead-time creates a distortion in the output voltage. Also, the various existing loads will create another source of distortion. It is then needed to apply some changes to the SPWM control. Fig. 6 shows the control diagram of the dc-ac full-bridge converter. This control diagram is mainly based in a PI controller and a feedforward component to enable a faster response of the system to the desired output voltage (v_O*). This control will change the reference sinusoidal waveform so that the desired output voltage is achieved. Fig. 7 shows simulation results of the produced voltage (v_O) and current (i_O) when the system supplies a non-linear load composed by a bridge rectifier with capacitive filter and a resistive load. It was also verified through simulation that the output filter inductor affects the output voltage. This situation is discussed in [16] and accordingly the filter inductor was dimensioned so that it does not affect the voltage control and creates a less distorted voltage, even when non-linear loads are supplied.

TABLE I
PERMANENT MAGNET SYNCHRONOUS GENERATOR (PMSG) CHARACTERISTICS

Parameters	Value	Unit
Rated Output Power	1800	W
Rated Rotation Speed	480	rpm
Rectified DC Current @ Rated Output	6	A
Required Torque @ Rated Power	44.5	N.m
Phase Resistance	5	Ω
Insulation	3.6	H Class
Generator configuration	3 phase (star)	ac
Design Lifetime	>20	years

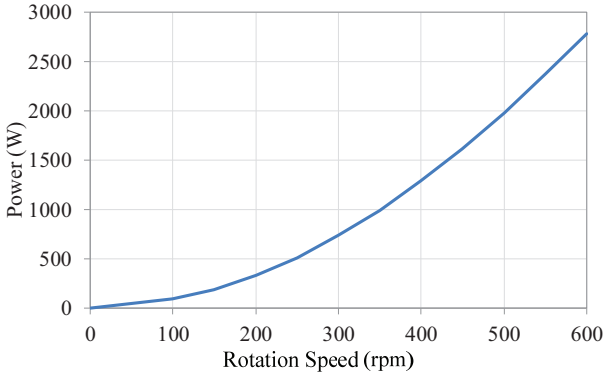

Fig. 8. Power curve of the PMS generator.

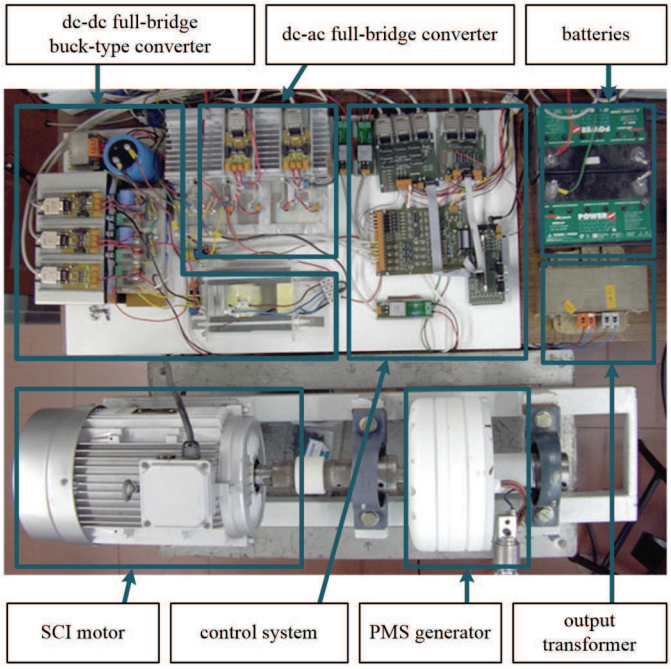

Fig. 9. Developed prototype

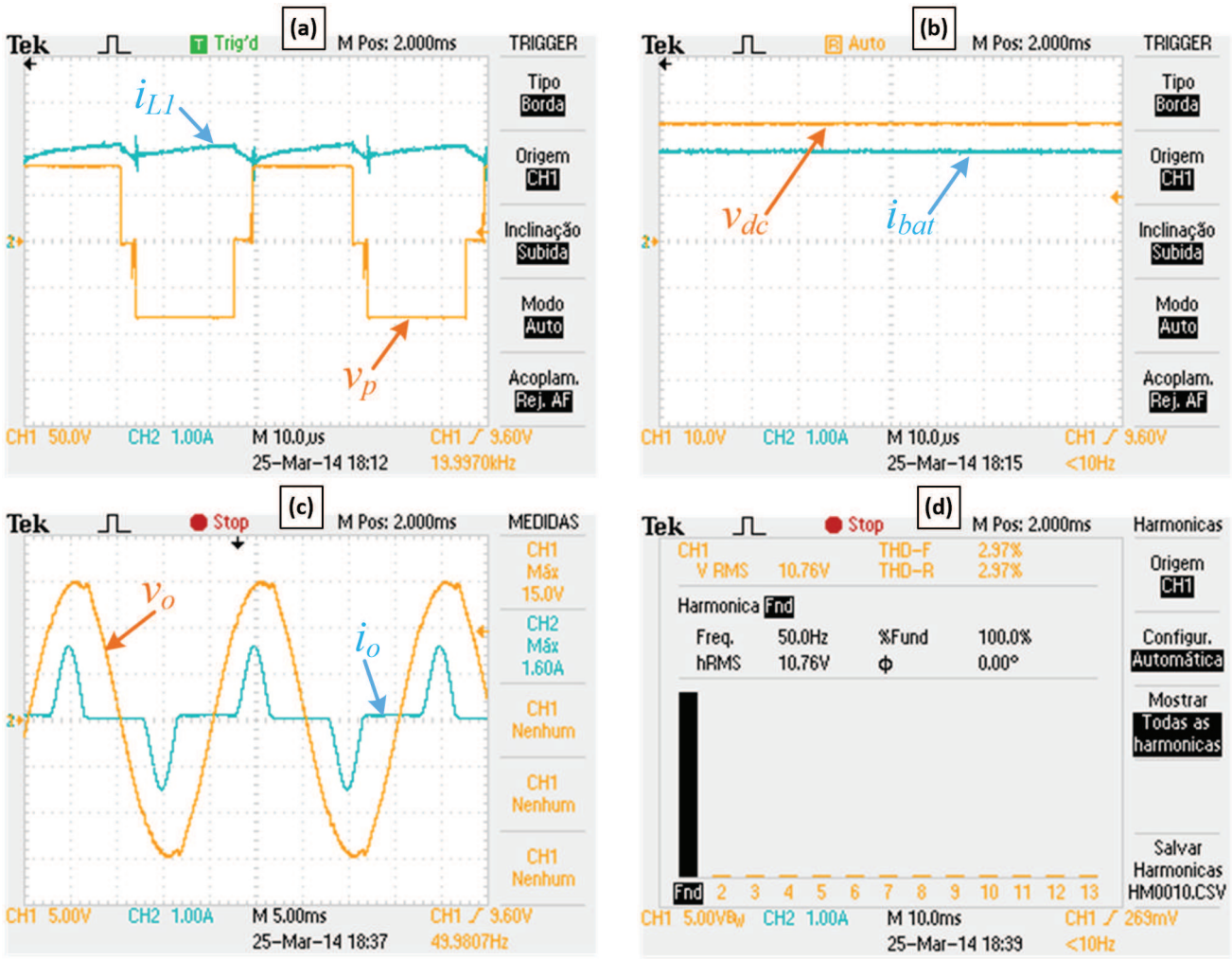

Fig. 10. Experimental results of the system using a non-linear load: (a) Transformer primary winding voltage (v_p) and inductor current (i_{L1}); (b) Dc link voltage (v_{DC}) and batteries current (i_{bat}); (c) Output voltage (v_o) and current (i_p); (d) Spectral diagram and THD% of the output voltage (v_o).

III. DEVELOPED PROTOTYPE

In this item, it is presented the developed prototype that allows the test of the system. This prototype is composed by three essential parts: the generator; the power converters; and the control system. These three parts are further described in detail.

A. Permanent Magnet Synchronous Generator

The generator used is a permanent magnet synchronous generator from *Ginlong Technologies* model *GL-PMG-1800* with the nominal characteristics presented in Table I. The power curve of the PMSG in function of its rotation speed is presented in Fig. 8. This was obtained through testing the extracted power at different speeds. This curve is important to verify the functionality of the MPPT since it allows verifying if the extracted power at a given rotation speed matches that exact point in the power curve. To emulate the wind it was used a squirrel cage induction motor (SCIM) with controlled rotation speed linked to the PMSG. This ac motor has a nominal power of 5.5 kW and a nominal velocity of 1000 rpm. The SCIM plus PMSG system is shown in Fig. 9.

B. Power Converters

As aforementioned, three power converters are used. The voltage and current in these power converters are measured through hall-effect sensors. To measure the voltage it was used sensors from *ChenYang* model *CYHVS5-25A*, and to obtain the current it was used sensors from *LEM* model *LA 100-P*. The ac-dc full-bridge rectifier is composed by a module with six diodes (nominal value of 800 V and 10 A) and by an output capacitive filter. This filter is used to reduce the voltage ripple of the output voltage in the rectifier and is composed by four capacitors of 470 µF and 385 V. The capacitors are connected in series and parallel, so that the final value of capacitance is 470 µF and the maximum voltage is 770 V. The dc-dc full-bridge buck-type converter is composed by four discrete IGBTs model *FGA120ANTD25N* (1200 V and 25 A), two diodes which compose the model *STTH100W06CW* (600 V and 50 A), a high frequency transformer with a 1.5:1 turns ratio with nominal power of 1800 kW, and an inductor of 500 µH. Two Absorbed Glass Mat (AGM) batteries of 33 Ah and 12 V connected in series are being used to test the prototype. After the initial tests, the number of batteries will be increased to

four. In the final application, lead-acid batteries of 1380 Ah and 4 V may be used in the system at higher power levels and in field environment [17]. The dc-ac full-bridge converter is composed by four MOSFETs model *STP210N75F6* (75 V and 120 A). A second order low-pass LC passive filter is used to connect this converter to the loads. Taking into account a compromise between the filter performance and component size, this filter inductance value is 70 μH and a capacitance of 40 μF. The used capacitance is split in two capacitors to smooth the gain response of the passive filter at the cut-off frequency and a damping resistor (R_D = 8 Ω) is used in series with one of them. It is also used a transformer with a 1:9.2 turns ratio with nominal power of 11 kVA, so that it is possible to achieve a voltage of 230 V to supply the loads.

C. Control System

The control system is composed by several circuits with analogue and digital signals. The aforementioned control algorithms were implemented using a DSP from *Texas Instruments* model *TMS320F28335*. The analogue voltages and currents needed to implement the control algorithms are converted to digital through an external ADC with bipolar inputs which is part of the signal conditioning circuit. The output PWM signals from the DSP are applied to the IGBTs/MOSFETs by means of *HCPL 3120* gate drivers.

IV. EXPERIMENTAL RESULTS

In this section, it is presented the experimental results obtained with the developed prototype. The complete developed prototype is presented in Fig. 9. After individually testing the converters, it was tested the full system with batteries, but without the output transformer. Fig. 10 (a) shows the voltage in the primary of the high frequency transformer and the current in the inductor of the dc-dc buck-type In Fig. 10 (b) is shown the controlled current applied to the batteries and the voltage in the dc link. Furthermore, in Fig. 10 (c) is shown the voltage and current applied to a nonlinear load composed by a bridge rectifier with capacitive filter and a resistive load. Finally, in Fig. 10 (d) it is shown harmonics contents of the voltage and the total THD of the voltage. According to [18] the total THD of the output voltage is within the stipulated values.

V. CONCLUSIONS

This paper presents the development of a system designed to extract the maximum power from a wind turbine and use it to supply an ac micro grid in isolated mode. These have been growing in interest for isolated places that are of difficult access with the main grid. The topology and control algorithm have been validated through simulation, using PSIM software, and through experimental results, using a developed prototype, which allowed the verification of the functionality of the system. For future work, it will be tested the MPPT control algorithms, evaluating their response in this system for different operating conditions.

ACKNOWLEDGMENT

This work has been supported by FCT – Fundação para a Ciência e Tecnologia within the Project Scope: Pest-OE/EEI/UI0319/2014.

REFERENCES

[1] M. H. Nehrir, C. Wang, K. Strunz, H. Aki, R. Ramakumar, J. Bing, Z. Miao, Z. Salameh, "A Review of Hybrid Renewable/Alternative Energy Systems for Electric Power Generation: Configurations, Control, and Applications," IEEE Trans. Sustain. Energy, vol.2, pp.392-403, Oct. 2011.

[2] Giorgio Corbetta, Thomas Miloradovic, "Wind in Power - 2013 European statistics," The European Wind Energy Association, Feb. 2014.

[3] "Renewable Energy Outlook - World Energy Outlook 2013," International Energy Agency, pp.196-232, Nov. 2013

[4] "2013 Half-Year Report," The European Wind Energy Association, Oct. 2013.

[5] J. A. Baroudi, V. Dinavahi, A. M. Knight, "A review of power converter topologies for wind generators," IEEE International Conference on Electric Machines and Drives, pp.458-465, May 2005.

[6] C. Zhe, J. M. Guerrero, F. Blaabjerg, "A Review of the State of the Art of Power Electronics for Wind Turbines," IEEE Trans. Power Electron., vol.24, pp.1859-1875, Aug. 2009.

[7] F. Giraud, Z. M. Salameh, "Steady-State Performance of a Grid-Connected Rooftop Hybrid Wind-Photovoltaic Power System with Battery Storage," IEEE Power Engineering Review, vol.21, pp.54-54, Feb. 2001.

[8] J. Hui, A. Bakhshai, P. K. Jain, "A hybrid wind-solar energy system: A new rectifier stage topology," IEEE APEC Applied Power Electronics Conference and Exposition, pp.155-161, 2010.

[9] J. Schonberger, R. Duke, S. D. Round, "DC-Bus Signaling: A Distributed Control Strategy for a Hybrid Renewable Nanogrid," IEEE Trans. Ind. Electron., vol. 53, pp. 1453-1460, Oct. 2006.

[10] T. Ackermann, "Wind Power in Power Systems," Second Edition, Wiley, 2012.

[11] D. A. Spera, "Wind Turbine Technology: Fundamental Concepts in Wind Turbine Engineering," Second Edition: American Society of Mechanical Engineers, 2009.

[12] E. H. Watanabe, M. Aredes, J. L. Afonso, J. G. Pinto, L. F. C. Monteiro, H. Akagi, "Instantaneous p-q Power Theory for Control of Compensators in Micro-Grids," International School on Nonsinusoidal Currents and Compensation, pp.17-26, June 2010.

[13] J. Benjanarasut, B. Neammanee, "The d-, q- axis control technique of single phase grid connected converter for wind turbines with MPPT and anti-islanding protection," IEEE International Conference Electrical Engineering/Electronics, Computer, Telecommunications and Information Technology pp.649-652, May 2011.

[14] Ruchika, R. Gour, P. Jain, Rashmi, R. Mittal, S. S. Deswal, "PMSG based isolated wind energy conversion system (WECS) for variable load," IEEE IICPE India International Conference on Power Electronics, pp.1-6, Dec. 2012.

[15] M. K. Kazimierczuk, "Pulse-width Modulated DC-DC Power Converters", Wiley, Sept. 2008.

[16] J. G. Pinto, V. Monteiro, H. Goncalves, B. Exposto, D. Pedrosa, C. Couto, J. L. Afonso, "Bidirectional battery charger with Grid-to-Vehicle, Vehicle-to-Grid and Vehicle-to-Home technologies," IEEE IECON Industrial Electronics Society, pp.5934-5939, Nov. 2013.

[17] Raylite Batteries, (online Mar. 2014). Available at: http://www.gwstore.co.za/site/store/index.php?type=view_product&id=270

[18] T. M. Blooming, D. J. Carnovale, "Application of IEEE STD 519-1992 Harmonic Limits," Conference Record of Annual in Pulp and Paper Industry Technical Conference, pp. 1-9, June 2006.